Metal-insulator and magnetic transition of NiO at high pressures

Xiao-Bing Feng
Department of Physics, Dalian Railway Institute, Dalian 116028, Peoples' Republic of China

N. M. Harrison
Department of Chemistry, Imperial College of Science, Technology and Medicine, London SW7 2AY, United Kingdom

(Received 11 August 2003; published 29 January 2004)

The metal-insulator transition and magnetic collapse of NiO under high pressures have been studied with the hybrid density functional (HDF) and the general-gradient approximation (GGA). Our results show that even in the intermediate coupling regime GGA does not take the correlation effects into account appropriately. HDF predicts that the transitions occur at much higher pressures than GGA does. Band broadening, covalence, and crystal-field effects are responsible for the changes of the electronic structure under high pressures.

DOI: 10.1103/PhysRevB.69.035114 PACS number(s): 71.15.Mb, 71.30.+h, 62.50.+p

I. INTRODUCTION

As a prototype of Mott insulators NiO has been intensively studied both experimentally and theoretically.[1] The discovery of high-temperature superconductivity in oxides containing CuO_2 planes has also revived interest in the metal-insulator (M-I) transitions in transition metal oxides. Some parent compounds of high-temperature superconductors (HTSC's) evolve from antiferromagnetic insulator into HTSC's upon hole doping.[2] On the other hand, the technical applications of antiferromagnetic materials also lead to the studies of magnetic multilayers and nanoparticles of NiO.[3]

Recently, Cohen *et al.* have carried out density-functional calculations on the magnetic collapses of some transition metal oxides under high pressure. They have found that some materials have magnetic collapse from high spin states to low spin states under the pressures reachable inside the Earth, and the magnetic collapse may have important effects on some geological phenomena.[4] They have calculated the magnetic moments with the Perdew-Wang general-gradient approximation (PWGGA) functional,[5] which gave significant increase of transition pressures over the local-density approximation (LDA) calculations.

Conventional LDA and GGA failed to predict the correct ground states of some strongly correlated electronic systems (SCES's).[6] Improvements over LDA and GGA are needed to understand these materials containing incomplete *d* or *f* shells. There are some theoretical approaches, such as LDA $+U$,[7] *GW* (Ref. 8) that can predict correct ground state. But the quantitative agreements with experiments are not satisfactory. LDA$+U$ scheme treated the Hubbard *U* term with Hartree-Fock mean-field method which may effect the precision of the results, also the choices of *U* are often in debate. The *GW* method, based on perturbative random-phase approximation, is computationally demanding.

In this paper we calculate the magnetic and M-I transitions of NiO under high pressures with the so-called B3LYP hybrid density functional.[9,10] The B3LYP functional has been successfully applied to strongly correlated systems and semiconductors of different bonding types.[11,12] The spurious self-interaction is reduced through the Hartree-Fock (HF) exchange, and the hybrid functional treats the correlation more appropriately by optimizing the coefficients of the various terms describing correlation effects. The energy gaps and magnetic moments from the B3LYP functional are in good agreement with experiments. B3LYP is more suitable for the study of magnetic collapse and M-I transition than GGA, the latter gave too small gaps and moments for NiO. GGA also failed to predict the correct ground state of the isostructural FeO and CoO.[13] It is argued that under high pressure the ratio of Hubbard *U* and bandwidth may decrease, so GGA may give more accurate results. Our calculations show that GGA still result in large error even at high electron density. The correlation effects are still playing an important role, even the average electron density has been more than doubled. Our results show that the magnetic collapse is preceded with the M-I transition and the transition pressures for magnetic collapse and M-I transition are much higher than GGA predicted. The band broadening, covalence, and crystal-field effects are responsible for the variation of the electronic structure of NiO under high pressures.

II. CALCULATION METHOD

The exchange-correlation functional in the B3LYP scheme is an admixture of the nonlocal HF exchange and the GGA local exchange-correlation functional.[9,10] The coefficients of the various terms are obtained by fitting the theoretical results to the thermochemical experimental data on some atoms and molecules. The application of B3LYP functional to periodic systems, such as semiconductors and SCES's, are quite successful. The unphysical self-interaction is reduced by the introduction of the nonlocal Hartree-Fock exchange. For semiconductors where the self-interaction is less important B3LYP also gives excellent energy gaps[12] while LDA$+U$ is expected to produce no significant improvements. The success of B3LYP suggests that it is a good start point for finding the exact energy functional. The B3LYP calculations in this paper have been implemented with CRYSTAL package.[14] In CRYSTAL atom-centered Gaussian basis sets are used to construct Bloch functions. The basis sets for Ni and O are taken from the previous unrestricted HF calculations on NiO.[15] They have the forms of 86-411/41 and 84-11 for Ni and O, respectively. The nonde-

TABLE I. The energy gaps Δ (in eV), magnetic moments μ (in μ_B), equilibrium lattice parameter a (in Å), bulk moduli B (in GPa), M-I transition pressure P_c, and magnetic collapse pressure P_m from different theoretical schemes (in TPa). The results from second lines for PWGGA and B3LYP are obtained with the Murnaghan equation of states. The LDA+U[7] and GW (Ref. 8) results are shown for comparisons. The experimental energy gap, magnetic moment, lattice constant and bulk modulus are taken from Refs. 19, 20, 17, and 18, respectively.

	Δ	m	a	B	P_c	P_m
PWGGA	1.3	0.66	4.183	201	0.68	0.71
			4.182	217		
LDA+U	3.1–3.4	1.56–1.74				
GW	3.7	1.56				
B3LYP	4.2	1.67	4.218	209	2.4	3.7
			4.225	198		
Expt	4.0–4.3	1.64–1.90	4.177	166–208		

fault auxiliary basis set for fitting the exchange-correlation potential has been used to obtain better results.[11] The tolerances for one-electron and two-electron integrals are set to 7, 7, 7, 7, and 14 to ensure high precision. Shrinking factor 8, which corresponds to 65 points in the irreducible part of the first Brillouin zone, has been used. The energy gap and moment are same as in the case of shrinking factor 12, which corresponds to 189 points in the irreducible part. The high pressure experiment on NiO shows that there is no structural transition up to about 150 GPa and the deformation from the rocksalt structure is small.[16] NiO has an AF_2 antiferromagnetic insulating ground state, in which spins are aligned on (111) planes with alternating spins on neighboring (111) planes. In this paper all calculations are carried out on an antiferromagnetic supercell built from the rocksalt structure. GGA calculations are also carried out for comparisons.

III. RESULTS AND DISCUSSION

The results of energy gaps, magnetic moments, lattice parameters, and bulk moduli from PWGGA and B3LYP are shown in Table I. For the PWGGA calculations the same basis sets and thresholds are used as in the B3LYP calculations. The energy gap and magnetic moment obtained from our B3LYP calculation are 4.2 eV and $1.67\mu_B$, respectively. These results are in accordance with the experiments[19,20] and previous B3LYP calculation.[11] LDA+U has given similar amplitudes for the magnetic moment as B3LYP, but the energy gap is significantly underestimated. To study the M-I transition it is crucial to use a theoretical scheme that could predict accurate energy gap, otherwise the transition pressure would be underestimated with small theoretical gaps. The lattice parameter and bulk modulus are obtained from the total energies at different volumes. As usual, B3LYP overestimates a little the lattice parameter. The bulk moduli from the second derivative and by fitting the Murnaghan equation of states[21] are all in agreement with the experiments.

The B3LYP projected densities of states (DOS's) of NiO in the ground-state antiferromagnetic phase without volume compression are shown in Fig. 1. In the octahedral crystal field the two e_g and three t_{2g} orbitals of Ni have the same partial DOS's, and the results shown in Fig. 1 are the total DOS's for the two types of d orbitals. At the top of the valence bands O p and Ni d partial waves have nearly the same spectral weights, while the low-lying conduction bands are mainly of Ni e_g character. From the t_{2g} DOS's one can see that the exchange splitting is about 1 eV, and the t_{2g} has much higher spectral weight than e_g orbitals. The peak distance between the spin-up and spin-down DOS's for e_g orbitals is about 10 eV, which is close to the GW and LDA $+U$ results.[5,6]

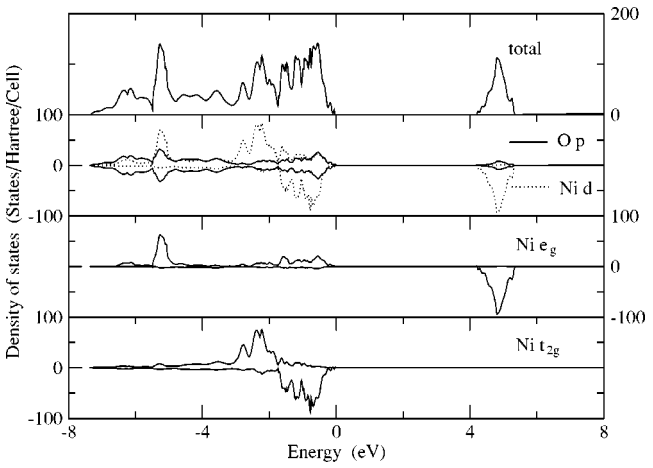

FIG. 1. The projected and total densities of states (DOS's) of NiO in AF_2 antiferromagnetic phase at atmosphere pressure. The DOS's for both spin components are shown for Ni e_g, Ni t_{2g}, and O p orbitals. The energies are measured from the top of the valence bands. The DOS's for spin-up and spin-down electrons are denoted by the positive and negative values, respectively. The projected DOS's for Ni $3d$ orbitals are for an spin-up Ni ion.

The electronic structure of NiO can be qualitatively understood in an ionic model and by taking the hybridization effects between the Ni $3d$ and O $2p$ states. Highly ionic characters in the bondings between transition metal ions and oxygen have been deduced for some transition metal monoxides, such as MnO (Ref. 22) and CoO.[23] Figure 2 shows the schematic plot for the ionization and affinity energies of NiO. The energy difference between occupied e_g and t_{2g} orbitals without hybridization with ligand oxygen ions is determined by $U_0-U'-\Delta_{CF}$, in which U_0 is the Coulomb repulsion energy between two electrons with opposite spins on the same d orbital, U' the repulsion energy for two electrons on different d orbitals, Δ_{CF} the crystal-field splitting. The many-body Hubbard U ,which is defined as the energy required to transfer an electron between two Ni ions, for Ni^{2+} in the octahedral crystal field is $U'-J+\Delta_{CF}$, in which J is the exchange integral between Ni $3d$ electrons of same spins. The exchange splitting between t_{2g} orbitals is $2J$. J is estimated to be about 1 eV. Due to the covalence effect between the cation and surrounding anions the antibonding $dp\sigma^*$ orbital has nearly the same energy as the t_{2g} orbital. The charge-transfer energy Δ is also greatly reduced from the bare one Δ_0.

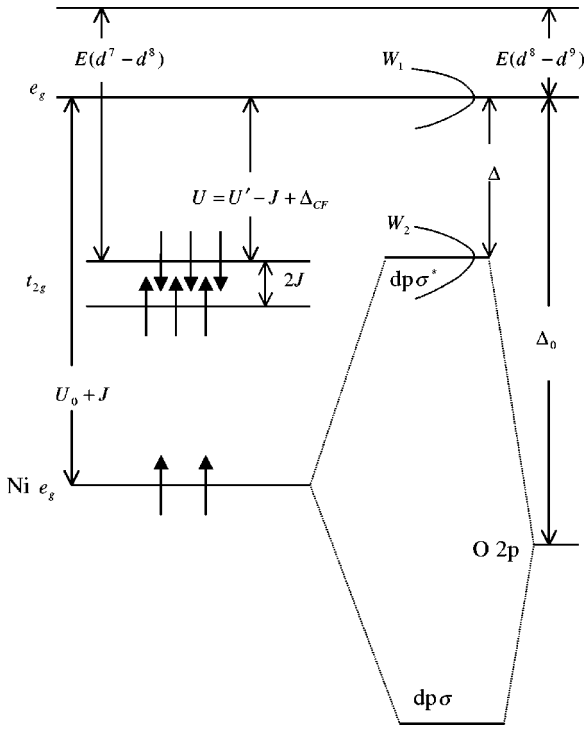

FIG. 2. The ionization and affinity energy levels for NiO from an ionic model. The hybridization between the Ni 3*d* and O 2*p* orbitals has also been shown. U_0 denotes the Coulomb interaction between two Ni 3*d* electrons on same orbitals, U' the interaction on different orbitals, J the exchange integral, Δ_{CF} the crystal splitting. Δ represents the charge-transfer energy, Δ_0 the bare charge transfer energy, i.e., the energy obtained by neglecting the hybridization interaction between Ni and O ions. The electron occupation is denoted by the up and down arrows.

From Fig. 1 one can see that the U and Δ are of the same size, this is in accordance with the previous conclusion based on the cluster method.[24] As will be seen later that the t_{2g} DOS's will move down due to the increase of Δ_{CF} when the material is compressed. Therefore, the energy gap can be expressed as

$$\Delta_g = U_0 + J - W - \left[\sqrt{\left(\frac{\Delta\epsilon}{2}\right)^2 + t^2} - \frac{\Delta\epsilon}{2} \right], \qquad (1)$$

where $W=(W_1+W_2)/2$ is the average bandwidth of the conduction and valence bands, $\Delta\epsilon=\epsilon_{e_g}-\epsilon_{2p}$ the energy difference between the Ni e_g and O 2*p* orbitals, t the transfer integral between Ni e_g and O 2*p* orbitals. The 10 eV interval between spin-up and spin-down e_g peaks is approximately given by $U_0+J+\Delta\epsilon/2+\sqrt{(\Delta\epsilon/2)^2+t^2}$. In addition to the bare on-site Coulomb repulsion, the covalence effect has also played an important role in forming the gap.

Figure 3 shows the variations of energy gaps and magnetic moments from B3LYP and PWGGA with volume compressing. For large volume compression ($>60\%$) there is a problem with the basis sets for oxygen. The large compression leads to linearly dependent basis sets. We removed the outermost sp shell for oxygen and reoptimized the 3*sp* shell exponent from 0.476 4 to 0.375. Both PWGGA and B3LYP

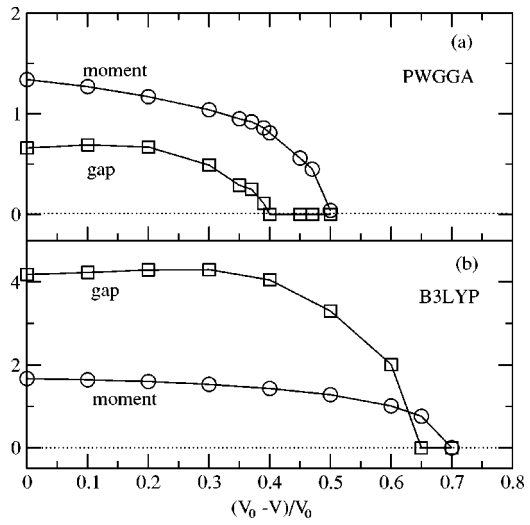

FIG. 3. The variation of moment (in μ_B, circles) and energy gap (in eV, squares) with volume compression. PWGGA (a) and B3LYP (b) results are shown. V_0 is the equilibrium volume of NiO.

give monotonic decreases of magnetic moments and nonmonotonic variations of energy gaps. PWGGA predicts M-I transition and magnetic collapse at about 40% and 50% volume compressions, respectively. These quantum phase transition points are significantly lower than the B3LYP results, about 65% and 70%. It was argued that with the increase of pressure the bandwidth W increases that the ratio U/W decreases. For NiO U/W decreased from 4.8 at zero pressure to 1.4 at the critical pressure, so the PWGGA results at high pressures should be more reliable than at zero pressure.[4] Our B3LYP calculations show that even at as large as 50% volume compression the GGA still generated significant error. The low transition pressures predicted by PWGGA results from the inappropriate description of exchange-correlation energy. The ratio $U/W=1.4$ means the system is in the intermediate coupling regime where correlation is still playing an important role in the electronic structure of the system.

To obtain the transition pressures the calculations are carried out for different unit-cell volumes to determine the transition points, then the pressures were obtained by the thermodynamics equation $P=-\partial E/\partial V$. The FIXINDEX option (i.e., same set of one-electron and two-electron integrals for slightly different volumes) has been used to reduce the numerical noise when the lattice parameters is changed. The real-space mesh technique is also used to reduce the errors caused by fitting the exchange-correlation potential with auxiliary Gaussian basis sets. In Fig. 4 the theoretical pressures from PWGGA and B3LYP at different volume compressions are compared with the experiment.[16] The results from the two schemes are all in good agreement with the experiment, but the electronic structures are quite different. The reason is that the pressures are determined by the total energies, which is a integral quantity, while the electronic structure is sensitively dependent on the local properties of the density functionals.

As can be seen in Table I the transition pressures from B3LYP are significantly higher than the results from PWGGA, which predicted higher magnetic collapse transi-

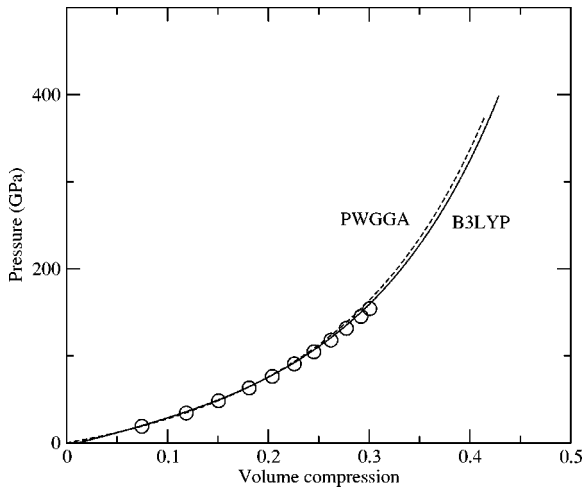

FIG. 4. The variation of the pressure with the volume compression, $(V_0-V)/V_0$. V_0 is the equilibrium volume. The solid and dashed lines represent the B3LYP and PWGGA results, respectively. The circles are the experimental results (Ref. 16).

tion pressure than LDA did. This trend can be understood by considering the correlation effects. The strong on-site Coulomb repulsion is in favor of localized magnetic moments and suppressing charge fluctuations. With taking more correlation effects into account one should obtain higher critical pressures for the both kind of transitions. The large pressure difference between the 65% and 70% volume compression may result from strong repulsion due to Coulomb and Pauli exclusion principle interactions when the ion cores are close enough.

Figure 5 shows the DOS's at 50% volume compression. One can see that the t_{2g} DOS's moved down from the top of valence bands due to increased crystal-field splitting. Thus, the low-energy properties of the material are determined by the antibonding $dp\sigma^*$ and the unoccupied e_g orbitals. At the top of the valence bands the e_g component is enhanced significantly over the O p orbital, making the material evolve from charge-transfer insulator towards Mott-Hubbard insulator.

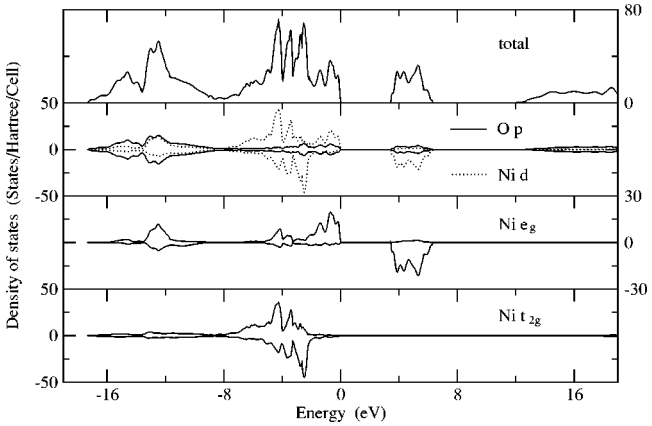

FIG. 5. The projected and total DOS's of NiO in AF_2 antiferromagnetic phase at 50% volume compression. The energies are measured from the top of the valence bands.

As expected, with increasing the pressure the transfer integrals t increases, which resulted in stronger band dispersions. In addition, when the material is compressed the energy difference $\Delta\epsilon$ increases due to the change of the Madelung potential. This effect together with the increased t would lead to larger separation between the bonding $dp\sigma$ and the antibonding $dp\sigma^*$ bonds. Such a trend is reflected in our results, as can be seen from Fig. 1 and Fig. 5. It is clear from Eq. (1) that the change of the gap results mainly from the last two terms. The bandwidth W increases monotonically with compressing, leading to narrowed gap. The last term comes from the covalence effect. Upon increasing pressure the effect may increase or reduce the gap, i.e., the effect is material dependent. From Fig. 3 one can conclude that at small compression this effect tends to enlarge the gap, which cancels the band broadening effect, leading to a slight change of the gap up to about 50% volume compression. With further increasing pressure the last term tends to approach an constant value, resulting in a rapid decrease of the gap. From the mechanism of M-I transition it is clear that adopting a theoretical scheme which could predict accurate gap values is essential in estimating the transition points, and the reason of the low transition pressures predicted by GGA is also evident.

As pointed out by Cohen *et al.*,[4] though the crystal-field splitting increased significantly it has no effect on the magnetic collapse. This is especially true for NiO because of the special Ni d^8 configuration. Our results indicate that the crystal field has also no effect on the M-I transition of NiO. The situation may be different if the e_g orbital lies above t_{2g}, such as in a tetrahedral coordination. Because of the strong hybridization between Ni e_g and O p orbitals the highest valence band would still be of $dp\sigma^*$ character. Thus, the increased crystal-field splitting would be an additional factor to enlarge the gap, resulting in a stronger nonmonotonic variation of the gap with increasing pressures.

Both GGA and B3LYP have predicted that the M-I transition is followed by a magnetic collapse. The magnetic collapse may be understood qualitatively with the extended Stoner theory.[4] In this scenario the small DOS's at the Fermi energy in the nonmagnetic solutions would drive the system from a magnetic to a nonmagnetic state. In the correlated systems, such as NiO, the on-site Coulomb repulsion also contributes to the Stoner's parameter, in addition to the contribution from the exchange interaction. This would make the magnetic transition occur at a higher pressure than the original Stoner's theory would predict. The results are in accordance with the Mott's standpoint that preformed moments are essential to open an Mott-Hubbard gap and that the moment is the sign of strong correlation in the Mott insulators.[1]

The low transition pressures predicted by GGA reflects the fact that GGA does not take the correlation into account appropriately even in intermediate coupling regime. Although GGA improves the equilibrium lattice parameters over LDA and B3LYP, it gives similar electronic structures as LDA does. For some strongly correlated electronic systems, such as $CaCuO_2$, CoO, FeO and etc., both LDA and GGA failed to predict the correct ground states of these materials. The application of B3LYP to $CaCuO_2$ (Ref. 25) and

CoO (Ref. 11) improves significantly the electronic structures over GGA. For $CaCuO_2$ GGA predicts that $CaCuO_2$ has a metallic ground state, while B3LYP predicts that the ground state of $CaCuO_2$ is an antiferromagnetic insulator. The B3LYP theoretical energy gap of $CaCuO_2$ is in excellent agreement with experiments. The energy bands across the Fermi energy, which are overlapping in the GGA results, get separated to form an energy gap. The mechanism of gap formation in B3LYP is quite similar to the LDA+U scheme.[26] This means that the strong on-site Coloumb interaction between 3d electrons is appropriately taken into account by B3LYP. In GGA the inherent self-interaction makes the orbitals of 3d electrons larger than they should be, hence the correlation is not properly taken into account, which often leads to underestimated energy gaps for correlated electronic systems. For NiO the underestimation of the energy gap by GGA results in lower M-I transiticon pressure than B3LYP predicts.

IV. CONCLUSION

To conclude, the magnetic and metal-insulator transitions of NiO at high pressures are investigated with the B3LYP and GGA density functional. Because of the better description for correlation effects the B3LYP hybrid functional gives transition pressures much higher than the ones obtained by GGA. In addition to band broadening effect the covalence effect has also played an important role in the M-I transition of NiO at high pressures.

ACKNOWLEDGMENTS

X.B.F. would like to thank B. Montanari for help with CRYSTAL and China Scholarship Council for financial support.

[1] See, for example, N.F. Mott, *Metal-Insulator Transitions* (Taylor & Francis, London, 1990).
[2] See, for example, *Physical Properties of High Temperature Superconductors I*, edited by D. M. Ginsberg (World Scientific, Singapore, 1989).
[3] See, for example, J. Nognes and I.K. Schuller, J. Magn. Magn. Mater. **192**, 203 (1999); R.H. Kodama, S.A. Makhlouf, and A.E. Berkowitz, Phys. Rev. Lett. **79**, 1393 (1997).
[4] R.E. Cohen, I.I. Mazin, and D.G. Isaak, Science **275**, 654 (1997).
[5] J.P. Perdew, in *Electronic Structure of Solids*, edited by P. Ziesche, and H. Eschrig (Academic, Verlag, Berlin, 1991); J.P. Perdew and Y. Wang, Phys. Rev. B **40**, 3399 (1989).
[6] W.E. Pickett, Rev. Mod. Phys. **61**, 433 (1989).
[7] A.B. Shick, A.I. Liechtenstein, and W.E. Pickett, Phys. Rev. B **60**, 10763 (1999); V.I. Anisimov, F. Aryasetiawan, and A.I. Liechtenstein, J. Phys.: Condens. Matter **9**, 767 (1997); S.L. Dudarev, A.I. Liechtenstein, M.R. Castell, G.A.D. Briggs, and A.P. Sutton, Phys. Rev. B **56**, 4900 (1997).
[8] S. Massidda, A. Continenza, M. Posternak, and A. Baldereschi, Phys. Rev. B **55**, 13 494 (1997).
[9] A.D. Becke, J. Chem. Phys. **98**, 5648 (1993).
[10] C. Lee, W. Yang, and R.G. Parr, Phys. Rev. B **37**, 785 (1988).
[11] T. Bredow and A.R. Gerson, Phys. Rev. B **61**, 5194 (2000).
[12] J. Muscat, A. Wander, and N.M. Harrison, Chem. Phys. Lett. **342**, 397 (2001).
[13] T.C. Leung, C.T. Chan, and B.N. Harmon, Phys. Rev. B **44**, 2923 (1991).
[14] V.R. Saunders, R. Dovesi, C. Roetti, M. Causà, N.M. Harrison, R. Orlando, and C.M. Zicovich-Wilson, Computer code CRYSTAL98 (University of Torino, Torino, 1998).
[15] M.D. Towler, N.L. Allan, N.M. Harrison, V.R. Saunders, W.C. Mackrodt, and E. Apra, Phys. Rev. B **50**, 5041 (1994).
[16] T. Eto, S. Endo, M. Imai, Y. Katayama, and T. Kikegawa, Phys. Rev. B **61**, 14 984 (2000).
[17] *CRC Handbook of Chemistry and Physics*, edited by D. R. Lide, (CRC, Boca Raton, 1998).
[18] E. Huang, K. Jy, and S.-G. Yu, J. Geophys. Soc. China **37**, 7 (1994).
[19] A. Fujimori and F. Minami, Phys. Rev. B **30**, 957 (1984); S. Hüfner, J. Osterwalder, T. Riesterer, and F. Hulliger, Solid State Commun. **52**, 793 (1984).
[20] B.E.F. Fender, A.J. Jacobson, and F.A. Wegwood, J. Chem. Phys. **48**, 990 (1968); A.K. Cheetham and D.A.O. Hope, Phys. Rev. B **27**, 6964 (1983); H.A. Alperin, J. Phys. Soc. Jpn. **17**, 12 (1962).
[21] F.D. Murnaghan, Proc. Natl. Acad. Sci. U.S.A. **30**, 244 (1944).
[22] A. Fujimori, N. Kimizuka, T. Akahane, T. Chiba, S. Kimura, F. Minami, K. Siratori, M. Taniguchi, S. Ogawa, and S. Suga, Phys. Rev. B **42**, 7580 (1990).
[23] W. Jauch and M. Reehuis, Phys. Rev. B **65**, 125111 (2002).
[24] J. Zaanen, G.A. Sawatzky, and J.W. Allen, Phys. Rev. Lett. **55**, 418 (1985).
[25] X.B. Feng and N.M. Harrison, http://arxiv.org/abs/cond-mat/0212588.
[26] V.I. Anisimov, J. Zaanen, and O.K. Andersen, Phys. Rev. B **44**, 943 (1991).